A Comparative Study of the Influence of Shift Factor Equations on Master Curve Construction

Nur Izzi Md. Yusoff[1+], Emmanuel Chailleux[2], and Gordon D. Airey[3]

Abstract: This paper evaluates the applicability of different shifting techniques for constructing complex modulus master curves using the time-temperature superposition principle (TTSP). A database of complex modulus results of unmodified bitumens, polymer modified bitumens (PMBs), bitumen-filler mastics, unaged and aged bitumens was used together with a Generalized Logistic Sigmoidal Model to assess the validity of seven different shifting approaches. Except for the *Laboratoire Central des Ponts et Chaussées* (LCPC) method, the construction of master curves was done using the Generalised Logistic Sigmoidal Model and non-linear least squares regression optimization with the aid of the Microsoft Excel Spreadsheet Solver function. The goodness-of-fit for the various shifting techniques and functions was assessed through graphical and statistical methods. From the study, it was found that a numerical shift approach using non-linear least squares produced the best fit between experimental and predicted data in terms of both graphical and goodness-of-fit statistics. The ranking of the other shifting techniques consisted of the LCPC approach, followed by the William, Landel and Ferry (WLF), Modified Kaelble, Viscosity Temperature Susceptibility (VTS), Arrhenius and Log-Linear methods. However, most of the equations are basically empirical and they are not expected to be strictly obeyed by any materials. Discrepancies were still evident, even for the better functions, for those materials that demonstrated a deviation from the thermorheological simplicity of the rheological behaviour as found for highly structured bitumens following high degrees of polymer modification and/or oxidative ageing.

Key words: Arrhenius equation, Generalised logistic sigmoidal model, Master curves, Shift factors, WLF equation.

Introduction

The rheological properties of bitumens are usually determined by means of dynamic mechanical analysis (DMA) using oscillatory type, dynamic shear rheometer (DSR) tests, generally conducted within the linear viscoelastic (LVE) region [1]. The principal viscoelastic coefficients that are obtained from the DSR are the magnitude of the complex modulus ($|G^*|$) and the phase angle (δ). $|G^*|$ can be defined as the ratio of maximum shear stress to maximum strain and provides a measure of the total resistance to deformation when bitumen is subjected to shear loading. It consists of two components, namely the storage (G') and loss (G'') moduli. The phase angle (δ or ϕ) is the phase, or time difference between stress and strain in harmonic oscillation and is an indication of the viscoelastic balance of the material behaviour.

Studies into the viscoelastic behaviour of bitumen have received increased interest from various researchers since the early 1990s, following the activities of the Strategic Highway Research Program (SHRP) [2-3]. The rheological properties of bitumens are normally presented in terms of $|G^*|$ and δ master curves together with the determination of shift factors associated with temperature shifting of

the rheological parameters. The temperature dependency of the viscoelastic behaviour of bitumens is indicated using shift factors and expressed as:

$$a_T = \frac{f_r}{f} \tag{1}$$

where a_T is the shift factor, f is the tested frequency and f_r is the reduced frequency at a reference temperature. Fig. 1 shows an example of how these shift factors at different temperatures are used to construct the $|G^*|$ and δ master curve at a particular reference temperature. Temperature dependency should not be confused with temperature susceptibly. Temperature dependency can be defined as a fundamental concept that indicates how the relaxation process within bitumen changes with temperature. Meanwhile temperature susceptibility is an empirical concept based on the change of consistency or hardness of bitumen with temperature.

The construction of master curves can be done using an arbitrarily selected reference temperature to which all rheological data are shifted. At the reference temperature, T_{ref}, the value of a_T is equal to one (log a_T is equal to zero). In general, several different a_T functions can be used to model the time-temperature equivalency relationship of bitumens and asphalt mixtures. Details of these functions will be discussed in full in section 2, where all the functions only involve horizontal line movements and do not take vertical shifts into account. The vertical shift, b_T, represents temperature induced density changes and involves shifts along the modulus axis. According to Wada and Hirose [4], since the temperature range of the experimental data for bitumen is usually relatively narrow, vertical shifts would only slightly modify results and moreover, the physical meaning of vertical shift is not a priori indent for bitumen, whose molecular structure is extremely complex. Furthermore, vertical shifts are highly dependent on the thermal history of the sample [5] and have been found to give a poor

---
[1] Dept. of Civil & Structural Eng., Fac. of Engineering & Built Environment, Universiti Kebangsaan Malaysia, 43600 Bangi, Selangor, Malaysia.
[2] LCPC, Division Matériaux et Structures de Chaussées, Laboratoire Central des Ponts et Chaussées, Route de Bouaye – BP 4129, F-44341 ,Bougueénais Cedex, France.
[3] Nottingham Transportation Engineering Centre, School of Civil Engineering, University of Nottingham, University Park, NG7 2RD, Nottingham, United Kingdom.
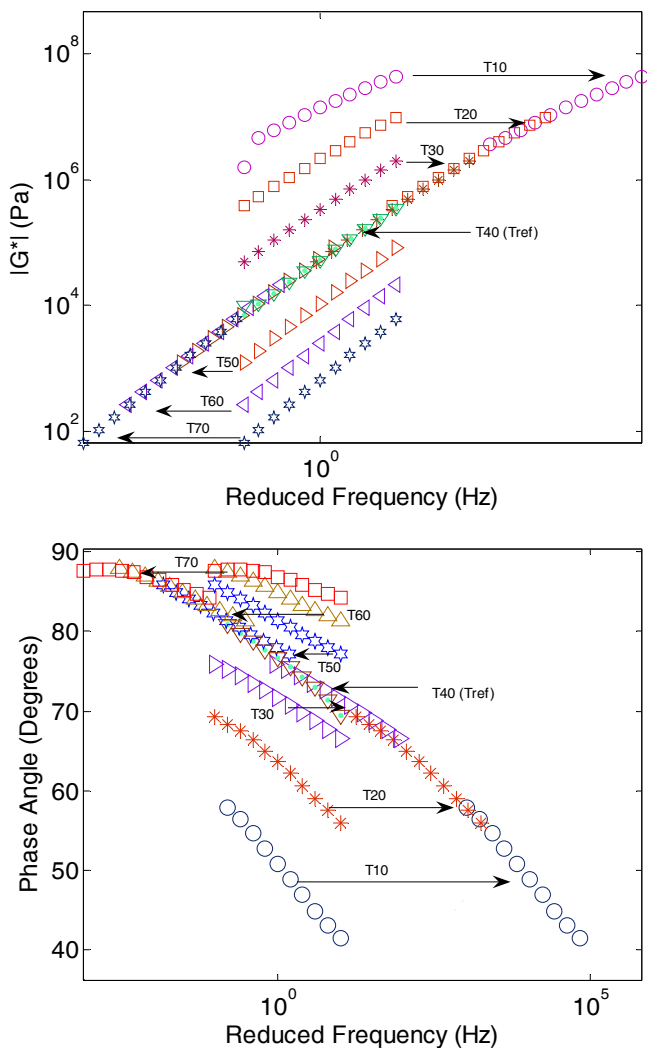[+] Corresponding Author: E-mail evxnim@nottingham.ac.uk

Fig. 1. Construction of the Complex Modulus and Phase Angle Master Curves.

prediction of density change upon heating for most bitumens [6].

A considerable number of studies have been conducted using various shift factor equations in order to construct smooth and continuous |G*| and δ master curves [7-13]. However, the different shift factor equations are usually used in isolation and no comparative study of the different shift factor functions or their applicability to different types of bituminous binders has been undertaken. This study was therefore conducted to assess the validity of several different shifting functions for constructing |G*| master curves of different bituminous binders by applying the time-temperature superposition principle (TTSP) [14].

Seven different shifting techniques or methods; namely a numerical, non-functional form shift approach, the Williams, Landel and Ferry (WLF) equation, a *Laboratoire Central des Ponts et Chaussées* (LCPC) approach, the modified Kaelble equation, a Viscosity Temperature Susceptibility (VTS) equation, an Arrhenius equation, and a Log-Linear approach have been used together with a large LVE rheological database held by the Nottingham Transportation Engineering Centre (NTEC). The NTEC database includes different combinations of unaged and aged samples of

unmodified bitumens, polymer modified bitumens (PMBs) and bitumen-filler mastics [15-18]. Correlations between the numerical, non-functional form (non-linear least squares) shift approach and other predicted functions were assessed using both graphical and goodness-of-fit statistical analysis methods.

Shift Factor Laws

Numerical, Non-linear Least Squares Shift

In the numerical, non-functional form shift approach, all the shift factors are solved simultaneously with the coefficients of the sigmoidal fitting function (described in section 3) using non-linear least squares fitting. This is achieved with the aid of the Microsoft Excel Spreadsheet Solver function without assuming any functional form for the relationship of a_T versus temperature as described by Pellinen *et al.* [9].

Williams, Landel and Ferry (WLF) Equation

The WLF equation, after it's discovers Williams, Landel and Ferry, has been widely used to describe the relationship between the a_T and temperature dependency and thereby determine the a_T of bitumens [19]:

$$\log a_T = \frac{-C_1\left(T - T_{ref}\right)}{C_2 + \left(T - T_{ref}\right)} \tag{2}$$

where T is temperature, T_{ref} is the reference temperature, C_1 and C_2 are taken as constants. The other parameters are as previously defined. This method is found to be applicable for both bitumens [20-22] and asphalt mixtures [23].

Modified Kaelble Equation

The Modified Kaelble equation can be thought of as a modification of the WLF equation and shown in the following form [3]:

$$\log a_T = \frac{-C_1\left(T - T_{ref}\right)}{C_2 + \left|T - T_{ref}\right|} \tag{3}$$

where the parameters are as defined in Eq. (2). Like the WLF equation, the C_1 and C_2 coefficients are used to minimise the error between measured and predicted |G*| data. The glass transition temperature (T_g) in the original equation has been replaced by T_{ref} since this study did not involve very low temperatures.

Arrhenius Equation

The Arrhenius equation can be described as the following:

$$\log a_T = C\left(\frac{1}{T} - \frac{1}{T_{ref}}\right) = \frac{0.4347\, E_a}{R}\left(\frac{1}{T} - \frac{1}{T_{ref}}\right) \tag{4}$$

where C is a constant, E_a is the activation energy (J/mol) and R is the ideal gas constant (8.314 J/mol.K). The other parameters are as previously defined. In the literature, different values, such as 10920,

13060 and 7680 K were reported for the constant C [24]. The Arrhenius expression requires only one constant to be determined, E_a, which describes the minimum energy needed before any intermolecular movement can occur.

Log-Linear Equation

Eq. (5) shows the form of the equation with the concept of reference temperature:

$$\log a \left(\frac{T}{T_{ref}} \right) = \beta \left(T - T_{ref} \right) \tag{5}$$

where β is the slope of the straight line relationship between log a_T and temperature [9]. As discussed by Garcia and Thompson [22], the Log-Linear equation is normally only used for asphalt mixtures. However, this equation has been used in this study as a comparison to the other methods.

Viscosity Temperature Susceptibility (VTS) Equation

In the Mechanistic-Empirical Pavement Design Guide (MEPDG), a_T was expressed as a function of binder viscosity to allow ageing over the life of the pavement to be considered using a global ageing model, developed by Mirza and Witczak [25]. Mirza and Witczak later devised the shift factor equation used in the MEPDG, termed the viscosity temperature susceptibility (VTS) equation [26]:

$$\log \ a_T \ = \ c \left(10^{A + VTS \ \log \ T_R} - 10^{A + VTS \ \log \ (T_R)_0} \right) \tag{6}$$

where T_R is temperature (Rankine), $(T_R)_0$ is the reference temperature (Rankine), A is the regression line intercept, VTS is regression line slope (called VTS coefficient) and c is a constant.

Laboratoire Central des Ponts et Chaussées (LCPC) Approach

Chailleux et al. [21] from the LCPC, France established a mathematical based procedure in order to construct master curves from dynamic measurements. Using the Kramers-Kronig relations and considering two close frequencies (f_i and f_j), they showed that:

$$\delta_{avr}^{(f_i, f_j)} \cdot \frac{2}{\pi} = \frac{\log \left(|G*(T, f_j)| \right) - \log \left(|G*(T, f_i)| \right)}{\log \left(f_j \right) - \log \left(f_i \right)} \tag{7}$$

where $\delta_{avr}^{(f_i, f_j)}$ is the average of the two phase angles measured at f_i and f_j (for temperature T) and $|G*(T, f)|$ represents the complex modulus. Note that the Kramers-Kronig relations are integral transform relationships between the real and imaginary parts of a complex function including the relation: $\delta(\omega) \approx \frac{\pi}{2} \cdot \frac{d \log |G*(\omega)|}{d \log (\omega)}$. A shift factor, $a_{(T1, T2)} = f_2/f_1$, exists as the TTSP is presumably valid. For two close temperatures, Eq. (7) can be rewritten as:

$$\delta_{avr}^{(T_1, T_2)}(f_2) \cdot \frac{2}{\pi} = \frac{\log \left(|G*(T_1, f_2)| \right) - \log \left(|G*(T_2, f_2)| \right)}{\log \left(a_{(T_1, T_2)} \right)} \tag{8}$$

where $\delta_{avr}^{(T_1, T_2)}$ is the average of two phase angles measured at T_1 and T_2 (for f_2). Shift factors can be calculated using Eq. (8) for close isotherms, at only one frequency. If measurements are carried out at temperatures T_1, $T_2...T_i$, $T_{i+1}...$, T_n, master curve construction related to a T_{ref} (with reference between 1 to n) can be performed using the cumulative sum of log ($a_{(T_i, T_{i+1})}$). Hence, the shift factor needed for an isotherm T_i according to T_{ref} will be:

$$\log(a_{(T_i, T_{ref})}) = \sum_{j=i}^{j=ref} \log (a_{(T_j, T_{j+1})}) \tag{9}$$

Combining Eqs. (8) and (9), allows the shift factors for the rheological data to be calculated as:

$$\log(a_{(T_i, T_{ref})}) = \sum_{j=i}^{j=ref} \frac{\log \left(|G*(T_j, f)| \right) - \log \left(|G*(T_{j+1}, f)| \right)}{\delta_{avr}^{(T_j, T_{j+1})}(f)} \times \frac{\pi}{2} \tag{10}$$

The calculation of a_T using the LCPC approach is based on linear viscoelasticity theory and derived solely from measurements of $|G*(j, T)|$ and δ (j, T) without the need for any adjustable coefficients.

Constructing Master Curves using the Generalized Logistic Sigmoidal Model

Master curves have been used by various researchers to describe and represent the LVE characteristics of bitumens and asphalt mixtures over a wide range of temperatures and frequencies. A large number of these studies have been devoted to the development of models to predict these rheological master curves. Among the various predictive models, the Sigmoidal Model used in the MEPDG can be considered to be one of the most popular. This model can be represented as follows [9, 24, 26]:

$$\log |G*(f, T)| = \delta + \frac{\alpha}{1 + e^{\beta + \gamma (\log f_r)}} \tag{11}$$

where $|G*(f, T)|$ is complex modulus as a function of frequency and temperature, $\log f_r$ is the log reduced frequency, δ is the lower asymptote, α is the difference between the values of the upper and lower asymptotes, β and γ are defined as shape coefficients. Fig. 2 shows a graphical definition of the sigmoidal function. Recently, the use of a Generalized Logistic Sigmoidal Model (or Richards Model) was recommended by Rowe et al. [3] to obtain a better fit of the non-symmetric curve of the master curve. This equation can be shown as:

$$\log |G*(F, T)| = \delta + \frac{\alpha}{\left(1 + \lambda \cdot e^{(\beta + \gamma (\log f_r))} \right)^{\frac{1}{\lambda}}} \tag{12}$$
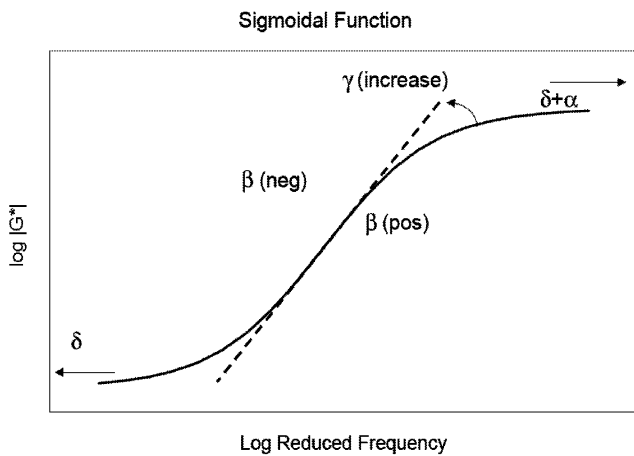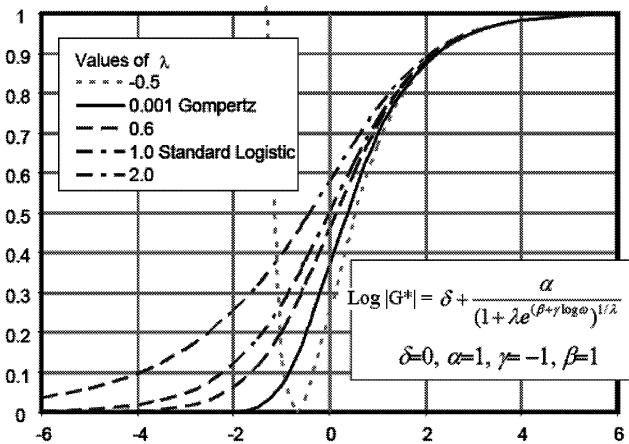
Sigmoidal Function

Fig. 2. Definition of Sigmoidal Function [9].

Fig. 3. Effect the Presence of λ Coefficient [3]

where the coefficients are as previously defined. The λ coefficient allows the curve to take a non-symmetrical shape (Fig. 3). When λ reduces to one, the above equation shrinks to the standard sigmoidal function as represented by Eq. (11) [3].

Details of the Fitting Procedure

The construction of the $|G^*|$ master curve was done with the aid of the Microsoft Excel Solver function, used for performing optimisation of data with non-linear least squares regression techniques. The procedure consisted of minimising the sum of square error (SSE) between numerical shift (hereafter called measured) and equation-based shift factor (hereafter called predicted) data as shown in Eq. (13):

$$SSE = \sum \frac{\left(\log\left|G_{exp}^*(f,T)\right| - \log\left|G_{pre}^*(a_T(T,T_{ref})\cdot f,T_{ref})\right|\right)^2}{\left(\log\left|G_{exp}^*(f,T)\right|\right)^2} \quad (13)$$

where $|G^*_{exp}(f, T)|$ is measured complex modulus, $|G^*_{pre}(f, T)|$ is predicted complex modulus, T is temperature (°C), T_{ref} is the reference temperature, f is frequency (Hz) and $a_T(T, T_{ref})$ is shift factor. In this study, the T_{ref} was arbitrarily taken as 25°C. By combining Eqs. (12) and (13), the following equation is obtained:

$$SSE = \sum \frac{\left(\log\left|G_{exp}^*(f,T)\right| - \left(\delta + \frac{\alpha}{\left(1+\lambda\cdot e^{\beta+\gamma(\log(a_T(T,Tref)\cdot f))}\right)^{\frac{1}{\lambda}}}\right)\right)^2}{\left(\log\left|G_{exp}^*(f,T)\right|\right)^2} \quad (14)$$

The coefficients α, δ, β, λ, and a_T (T, T_{ref}) are fitted in the minimization procedure between measured and predicted data. For the shift factor a_T (T, T_{ref}) coefficient, the various expressions described in section 2 were used. For the numerical shift and LCPC methods, the only parameters used to minimise the error between measured and predicted $|G^*|$ data are those from the Generalised Logistic Sigmoidal Model. In contrast, for the other functions, such as the WLF, Modified Kaelble, Arrhenius, VTS and Log-Linear equations, their coefficients were used together with the master curve model. For instance, when the WLF equation is used to represent the shift factor function, Eq. (14) becomes:

$$SSE = \sum \frac{\left(\log\left|G_{exp}^*(f,T)\right| - \left(\delta + \frac{\alpha}{\left(1+\lambda\cdot e^{\beta+\gamma\left(\frac{-C_1(T-Tref)}{C_2+(T-Tref)}+\log f\right)}\right)^{\frac{1}{\lambda}}}\right)\right)^2}{\left(\log\left|G_{exp}^*(f,T)\right|\right)^2} \quad (15)$$

The coefficients that need to be determined are now α, δ, β, λ, C_1 and C_2. The Solver function, together with initial seed values for the coefficients, is used to obtain the optimum values of the coefficients using a number of minimisation runs [27]. When no further changes are observed, the iteration process is terminated and the final values quoted for the coefficients.

However, it should be noted that this study only focuses on the comparison between measured and predicted a_T values and does not consider anomalies that can be seen in the construction of some of the $|G^*|$ master curves. This refers particularly to anomalies associated with the presence of highly crystalline bitumens (wax content > 7%), structured bitumen with high asphaltenes content and highly PMBs (> 5% polymer content). Fig. 4 shows an example of the WLF shift factor function for one of the unmodified bitumen samples used in this study. Fig. 5 subsequently depicts $|G^*|$ and δ master curves constructed using the above shift factors.

Goodness-of-Fit Statistics

Several statistical methods have been used in this study to indicate the goodness-of-fit between measured and predicted data [28-30].

Standard Error Ratio (S_e/S_y)

The standard error of estimation, S_e, and standard error of deviation, S_y, can be defined as follows:

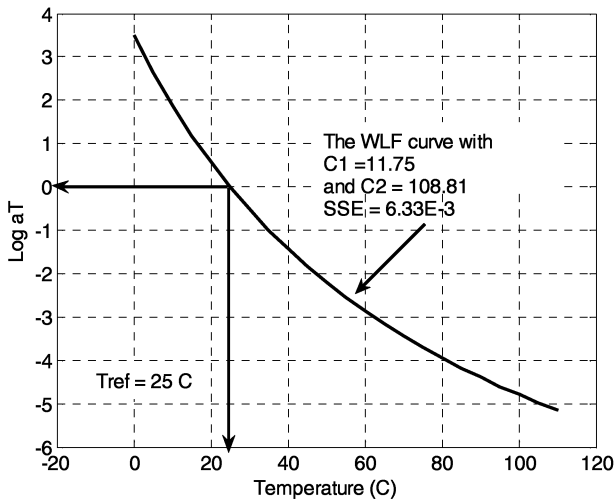$$S_e = \sqrt{\frac{\sum\left(Y - \hat{Y}\right)^2}{(n-k)}} \quad (16)$$

Fig. 4. An Example of WLF Shift Factor Curves for Unmodified Bitumen.
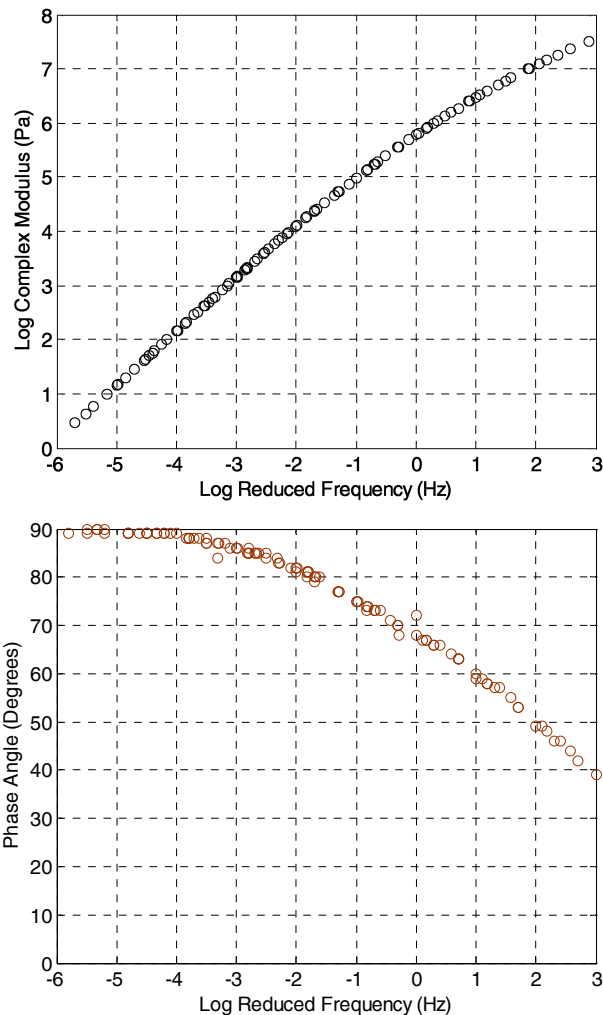

Fig. 5. Complex Modulus and Phase Angle Master Curves.

and

$$S_y = \sqrt{\frac{\sum (Y - \overline{Y})^2}{(n-1)}} \qquad (17)$$

Table 1. Criteria of the Goodness-of-fit Statistics [28].

Criteria	R^2	S_e/S_y
Excellent	≥ 0.90	≤ 0.35
Good	$0.70 - 0.89$	$0.36 - 0.55$
Fair	$0.40 - 0.69$	$0.56 - 0.75$
Poor	$0.20 - 0.39$	$0.76 - 0.89$
Very Poor	≤ 0.19	≥ 0.90

where n is sample size, k is number of independent variables in the model, Y is measured a_T, $\hat{Y}$ is predicted a_T and $\overline{Y}$ is mean value of measured a_T.

The Coefficient of Determination, R^2

The coefficient of determination, R^2 is determined as follows:

$$R^2 = 1 - \frac{(n-k)}{(n-1)} \cdot \left(\frac{S_e}{S_y} \right)^2 \qquad (18)$$

where the coefficients are as previously defined. For the perfect fit, $R^2 = 1$. The criteria for the S_e/S_y and R^2 goodness-of-fit statistics are shown in Table 1 [28].

The Discrepancy Ratio, r_i

The discrepancy ratio, r_i is calculated as follows:

$$r_i = \frac{a_{T_{p_i}}}{a_{T_{m_i}}} \qquad (19)$$

where $a_{T_{p_i}}$ and $a_{T_{m_i}}$ are the predicted and measured a_T, respectively. The subscript i denotes the data set number. For a perfect fit, r_i is equal to 1.

The Mean Normalized Error (*MNE*)

The mean normalised error (*MNE*) is determined as follows:

$$MNE = \frac{100}{J} \sum_{i=1}^{J} \left| \frac{a_{T_{p_i}} - a_{T_{m_i}}}{a_{T_{m_i}}} \right| \qquad (20)$$

where J is the total number of the data points and for a perfect fit, *MNE* is equal to 0.

The Average Geometric Deviation (*AGD*)

The average geometric deviation (*AGD*) is defined as:

$$AGD = \left(\prod_{i=1}^{J} \widetilde{R}_i \right)^{\frac{1}{J}}, \; \widetilde{R}_i = \begin{cases} a_{T_{p_i}} / a_{T_{m_i}} & \text{for} \quad a_{T_{p_i}} \geq a_{T_{m_i}} \\ a_{T_{m_i}} / a_{T_{p_i}} & \text{for} \quad a_{T_{p_i}} < a_{T_{m_i}} \end{cases} \qquad (21)$$

For a perfect fit, *AGD* is equal to 1.

Experimental Data Set

A collection of DSR tests, conducted in the LVE response region, of unaged and aged unmodified bitumens, polymer modified bitumens (PMBs) and bitumen-filler mastics has been used in this study to verify the validity of the shift factor equations. Details of the physical properties some of the tested binders and mastics can be found in the following references [15-17]. For example, the penetration and softening point values of unaged PMBs decrease and increase with increasing polymer content and subsequent polymer modification. The increase of binder hardness can be directly attributed to the stiffening effect caused by the addition of polymer (ethylene vinyl acetate (EVA) and styrene butadiene styrene (SBS) polymers). A similar observation was made for the aged PMBs samples.

All the binders and mastics were subjected to both amplitude (strain) as well as frequency sweeps to; firstly, establish the linearity region of response of the material and subsequently to determine their LVE rheological properties. The frequency sweep tests were performed under controlled strain loading conditions using frequencies between 0.1 to 10 Hz at 5°C temperature intervals between 5 and 75°C. Tests at lower temperatures (generally between 5 and 35°C) were undertaken with a 8 mm diameter and 2 mm gap testing geometry and at higher temperatures (generally between 25 to 75°C) with a 25 mm diameter and 1 mm gap testing geometry.

At low frequencies and/or high temperatures, the PMBs and bitumen-filler mastics show higher $|G^*|$ values compared to the unmodified bitumens. On the other end, at high frequencies and/or low temperatures, the curves approach a limiting value, known as the glassy modulus (G_g), at 1×10^9 Pa for unaged and aged unmodified bitumens and PMBs. However, for the unaged and aged bitumen-filler mastics, the G_g values vary, depending on the percentage and a type of mineral fillers used. This phenomenon occurs due to the existence of physical interaction in a mixture. In addition, the presence of polymer and mastics increase the elastic response (reduced δ) as temperature increased. Details of the LVE rheological properties of the binders and mastics can be found in the following references [15-17].

Results and Discussion

Graphical Comparison

Comparisons between predicted (shift factor functions) and measured (numerical) shift factors are shown graphically in Figs. 6-7. These plots are intended to visually and qualitatively show the agreement between measured and predicted values and to display any errors associated with the predictive equations and/or material combinations [31]. The predictive equations consist of the WLF, Modified Kaelble, Arrhenius, Log-Linear, VTS and LCPC functions/procedures. The measured shift factor data consists of the numerical, non-functional form shift approach. This approach used non-linear least squares fitting with the aid of the Microsoft Excel spreadsheet Solver function to simultaneously determine the coefficients associated with Eq. (15). As discussed by Pellinen et al. [9], the numerical shift approach produces the best results in terms

of data shifting flexibility due to the fact that this method has the highest degree of freedom. This method, however, has no physical meaning (or functional form) and has simply been used as a comparison to the other shift factor methods.

The numerical shifts are always plotted on the x-axis (Figs. 6-7). A combination of comparisons between measured and predicted a_T for the unaged unmodified bitumens, PMBs and bitumen-filler mastics are shown in Fig. 6. Fig. 7 represents the combinations of these samples that have undergone various ageing processes. From Fig. 6, it can be seen that the WLF and Arrhenius equations show the best results with the predicted a_T values being close to the equality line. Reasonably good correlations can also be seen for the VTS and Modified Kaelble methods. The WLF equation, originally derived from the empirical Doolittle equation relating fractional free volume theory to temperature, is clearly applicable for all bituminous materials. As mentioned by Dealy and Larson [32], the WLF equation generally provides a better fit of the data at temperatures closer to the glass transition temperature, T_g. However, the results in Figs. 6-7 also show that the WLF equation is also applicable at higher temperatures for bituminous binders.

Rowe et al. [3] found that the Modified Kaelble method was applicable for asphalt mixtures particularly at low temperatures. This method shows a sigmoidal type behaviour which does not result in excessively high values of a_T as the temperature reduces. However, it is observed that the Modified Kaelble method underestimates the unmodified bitumens at low temperatures compared to the original WLF equation. The Log-Linear equation, as expected, showed the lowest correlation between measured and predicted a_T. This expected result could relate to the fact that the equation is only suitable for the construction of asphalt mixture master curves. The VTS equation appears to be unsuitable for predicting a_T of the unmodified bitumens at low frequencies and/or high temperatures. Finally, the LCPC method showed a dispersion of predicted a_T data particularly for the unaged bitumen-filler mastics. Similar findings were observed by Chailleux et al. [21] for asphalt mixture where anomalies had been seen particularly at high frequencies. From their study, they found that the dispersion of a_T data normally occurs at the transition between the highest tested frequency for a particular temperature and the lowest tested frequency for the next (higher) temperature. The low data quality can be partly attributed to compliance errors associated with the measurement of δ and the subsequent use of the δ function [1, 33].

Fig. 7 shows a comparison between measured and predicted a_T of the different a_T equations for the aged unmodified bitumens, PMBs and bitumen-filler mastic samples. The results show a larger discrepancy between the predicted and measured a_T values, particularly at both lower and higher temperatures. The WLF, Modified Kaelble, VTS, LCPC and Arrhenius methods produced almost identical results when comparing the measured and predicted a_T. The Log-Linear equation slightly overestimates the measured a_T. In general, it is observed that all the models suffer from a similar drawback where they are unable to accurately predict the a_T data. This lack of agreement between measured and predicted a_T particularly for the aged mastics and PMBs can be attributed to the increased complexity of the rheological response of the materials

Fig. 6. Comparison between a_T (Numerical Shift) and a_T (Predicted) of Different Shift Factor Equations for the Unaged Samples ($T_{ref} = 25^{o}$C).

following oxidation and increased structuring. Moreover, most of the a_T equations (functions) are empirical and are therefore unable to account for changes in the physicochemical properties of the materials after ageing.
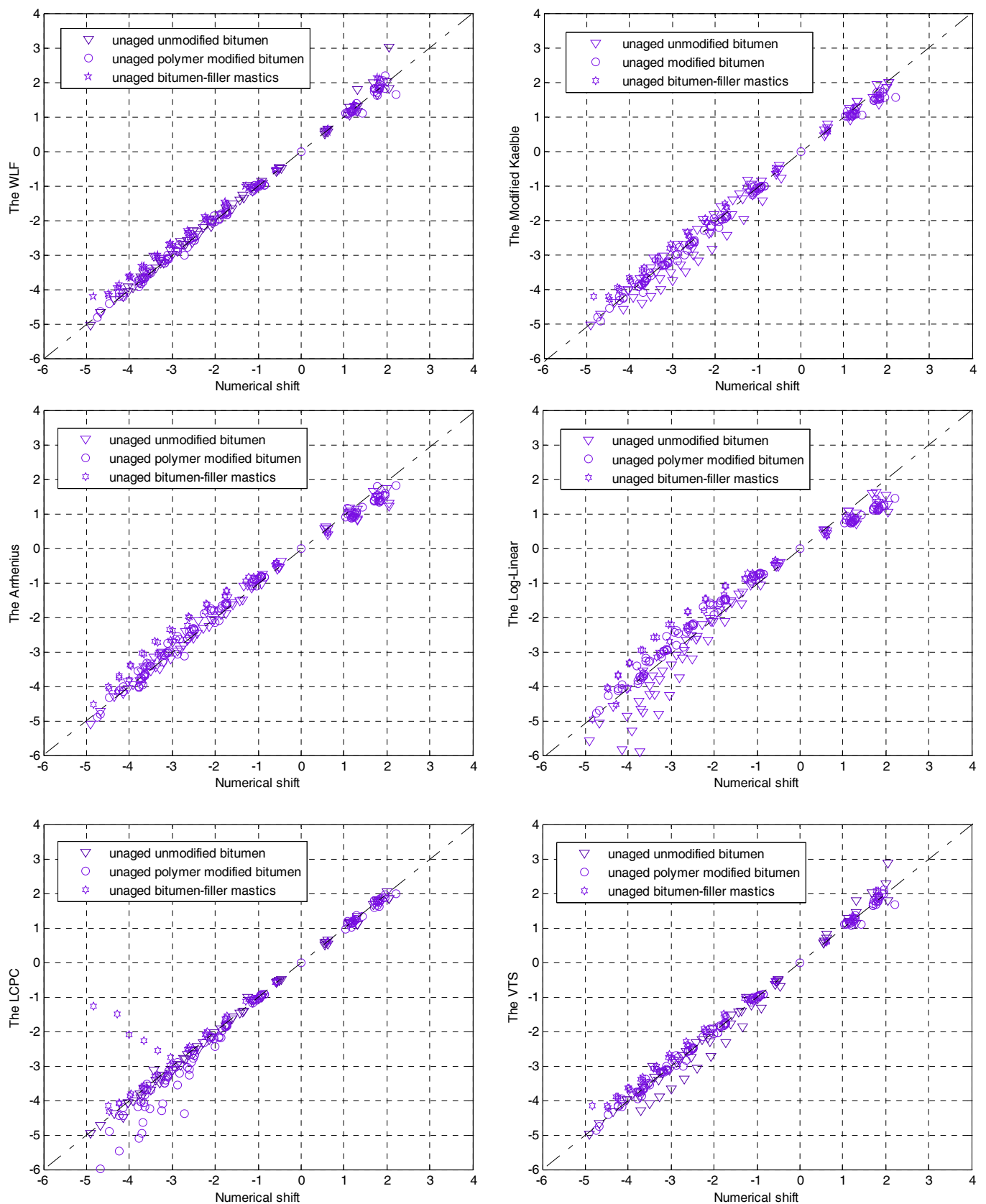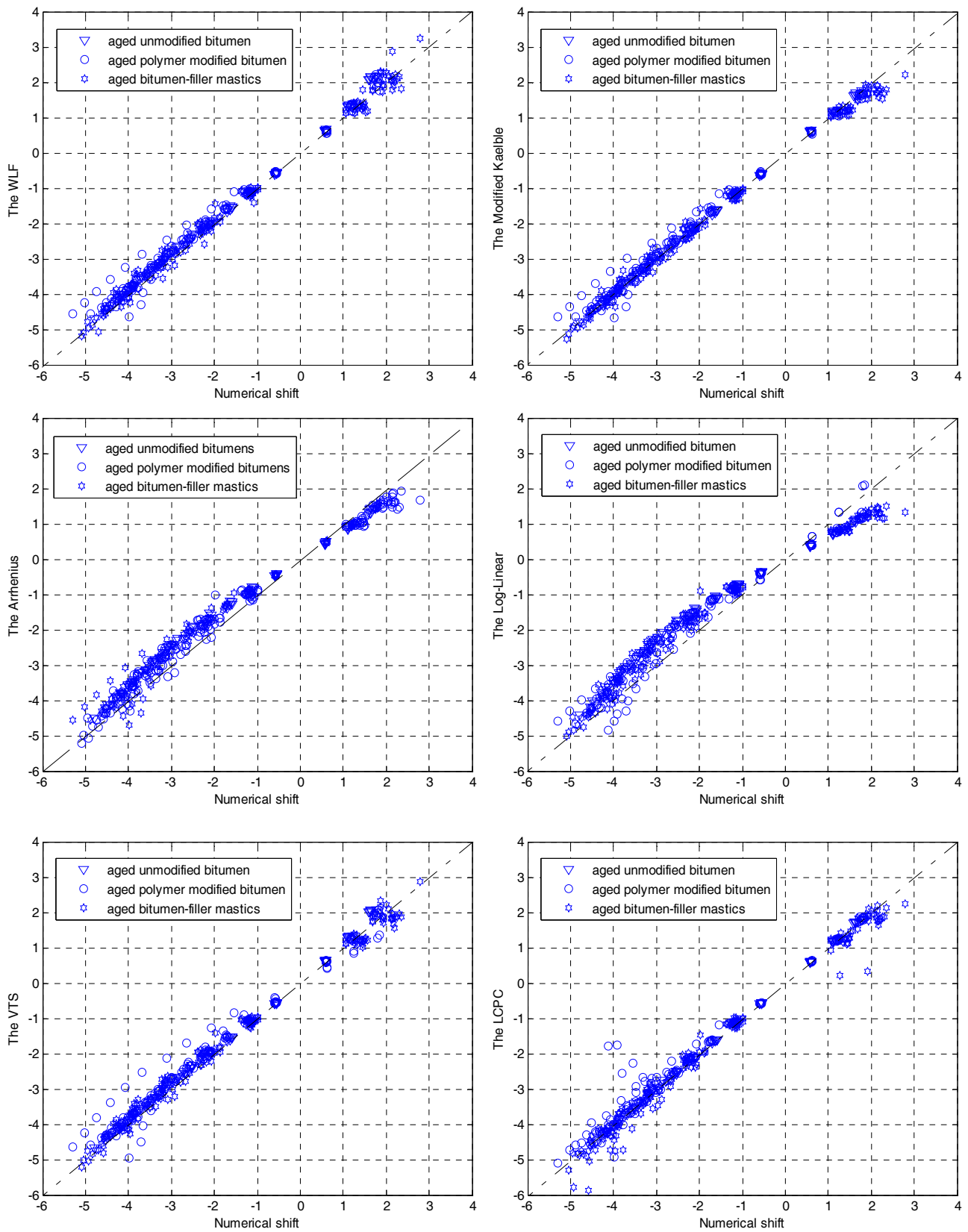
Fig. 7. Comparison between a_T (Numerical Shift) and a_T (Predicted) of Different Shift Factor Equations for the Aged Samples ($T_{ref} = 25^{o}$C).

Goodness-of-Fit Statistics

Tables 2-3 show the S_e/S_y and R^2 goodness-of-fit statistics associated

with the different a_T equations on unaged and aged samples. The unaged PMBs and bitumen-filler mastics shifted by means of the LCPC method show good correlations between measured and

Table 2. Summary of the S_e/S_y, R^2, r_i, MNE and AGD Goodness-of-fit for Unaged Samples.

| Method | Binders | n | S_e/S_y | R^2 | Data in Range of Discrepancy Ratio, r_i (%) | | | | | MNE | AGD |
					0.98 - 1.02	0.96 - 1.04	0.94 - 1.06	0.92 - 1.08	0.90 - 1.10		
WLF		71	0.086	0.993	42.25	60.56	73.24	81.69	87.32	5.10	1.05
Modified Kaelble		71	0.177	0.969	12.86	20.00	30.00	35.71	47.14	14.07	1.14
Arrhenius	Unmodified	71	0.110	0.988	23.94	38.03	50.70	60.56	69.01	8.58	1.10
Log-Linear	Bitumens	71	0.307	0.906	7.04	15.49	26.76	38.03	46.48	16.41	1.18
VTS		71	0.147	0.979	32.39	52.11	56.34	60.56	64.79	10.12	1.10
LCPC		71	0.057	0.997	40.85	54.93	78.87	84.51	90.14	4.29	1.04
WLF		106	0.050	0.998	40.95	71.43	82.86	90.48	93.33	3.67	1.04
Modified Kaelble		106	0.085	0.993	5.71	32.38	50.48	58.10	68.57	7.98	1.08
Arrhenius	PMBs	106	0.106	0.989	11.43	28.57	38.10	52.38	58.10	10.09	1.12
Log-Linear		106	0.173	0.970	3.81	11.43	14.29	16.19	21.91	17.45	1.22
VTS		106	0.050	0.998	45.71	69.52	84.76	92.38	93.33	3.51	1.04
LCPC		106	0.410	0.831	13.33	31.43	49.52	58.10	69.52	11.36	1.10
WLF		42	0.138	0.981	4.76	14.29	16.67	30.95	61.91	9.27	1.11
Modified Kaelble		42	0.110	0.988	0.00	9.52	33.33	69.05	76.19	7.66	1.08
Arrhenius	Bitumen-filler	42	0.217	0.953	0.00	2.38	7.14	9.52	14.29	19.13	1.24
Log-Linear	Mastics	42	0.262	0.932	4.76	7.14	11.91	11.91	16.67	24.09	1.33
VTS		42	0.133	0.983	11.91	14.29	21.43	45.24	71.43	8.47	1.09
LCPC		42	0.397	0.839	19.05	47.62	61.91	73.81	83.33	9.68	1.14

Table 3. Summary of the S_e/S_y, R^2, r_i, MNE and AGD goodness-of-fit for aged samples

| Method | Binders | n | S_e/S_y | R^2 | Data in Range of Discrepancy Ratio, r_i (%) | | | | | MNE | AGD |
					0.98 - 1.02	0.96 - 1.04	0.94 - 1.06	0.92 - 1.08	0.90 - 1.10		
WLF		71	0.091	0.992	15.49	43.66	64.79	74.65	84.51	6.99	1.07
Modified Kaelble		71	0.021	0.999	56.34	81.69	90.14	91.55	95.78	2.56	1.03
Arrhenius	Unmodified	71	0.200	0.960	0.00	0.00	0.00	5.63	15.49	17.20	1.21
Log-Linear	Bitumens	71	0.276	0.924	0.00	0.00	0.00	4.23	8.45	25.46	1.35
VTS		71	0.081	0.994	12.68	52.11	66.20	83.10	85.92	6.13	1.06
LCPC		71	0.022	0.999	70.42	85.92	94.37	100.00	100.00	1.84	1.02
WLF		140	0.136	0.982	9.29	28.57	43.57	61.43	74.29	8.14	1.09
Modified Kaelble		140	0.110	0.988	27.14	50.71	65.71	74.29	81.43	5.75	1.06
Arrhenius	PMBs	140	0.155	0.976	6.70	16.76	22.35	30.73	39.67	13.94	1.17
Log-Linear		140	0.240	0.946	5.00	7.14	12.86	17.14	21.43	21.07	1.28
VTS		140	0.168	0.972	9.29	23.57	39.29	54.29	65.71	9.98	1.12
LCPC		140	0.180	0.968	37.14	57.86	75.00	84.29	86.43	5.48	1.06
WLF		179	0.085	0.993	26.26	45.25	62.01	74.30	79.33	6.57	1.07
Modified Kaelble		179	0.087	0.992	31.84	49.72	60.34	67.04	73.74	6.88	1.08
Arrhenius	Bitumen-filler	179	0.209	0.957	1.43	3.57	7.14	12.86	20.00	17.21	1.21
Log-Linear	mastics	179	0.222	0.951	3.91	10.06	15.64	18.99	22.91	21.57	1.29
VTS		179	0.097	0.991	18.99	37.43	49.72	59.22	64.25	8.05	1.09
LCPC		179	0.128	0.984	23.46	43.58	56.43	63.13	71.51	8.06	1.10

predicted a_T data. The S_e/S_y and R^2 goodness-of-fit parameters tend to indicate excellent correlation between measured and predicted a_T data for most all tested material and shift factor combinations. However, according to Tran and Hall [28], the correlation coefficient, R^2, is not always a reliable coefficient to measure the goodness-of-fit for non-linear regression analysis. In addition, it is questionable whether S_e/S_y is a good tool to perform a comparison between measured and predicted data. For example, in the case of $|G*|$ measurements over a large temperature range, the standard deviation (S_y) has no meaning. S_y is only scientifically founded for

multiple $|G*|$ measurements under the same experimental condition (i.e. at one temperature and one frequency). In this case, S_y corresponds to the average distance between the mean value and all the experimental data.

Therefore, a more microscopic statistical analysis is needed and subsequently the discrepancy ratio (r_i), mean normalized error (MNE) and average geometric deviation (AGD) goodness-of-fit statistics are introduced, as shown in Tables 2-3. As discussed by Wu *et al.* [30], it is not straightforward to determine which method performs best since different statistical methods lead to different

rankings. The discrepancy ratio, r_i (%) is used to observe the predicted data's tabulation from the equality line with a perfect value being one. When the r_i is larger or smaller than one, it measures how much wider the prediction interval has to be to cover the observed number of cases [30]. A smaller range means a closer range to the perfect agreement. In this study, an interval of $1 \pm (0.02, 0.04, 0.06, 0.08 \text{ and } 0.10)$ is used. An example is shown for the WLF equation of unmodified bitumens, with an understanding that the commentary applies to other equations, both on the unaged and aged samples. A value of 0.98–1.02 represents an area where the ratio between predicted and measured a_T data is taken 0.02 to each left and right side from the equality line. It is observed that the r_i is equal to 42.25%. When the region widens with 0.02 more on each right and left sides (now the range between 0.96–1.04), another 18.31% of data is included. In this range, the data's tabulation increased up to 60.56%. A similar process is repeated for the r_i in the range of 0.94–1.06, 0.92–1.08 and 0.90–1.10, resulting the data's tabulation up to 73.24, 81.69 and 87.32%. In general, the improvement in r_i happens in all ranges. The *MNE* is related to the overall discrepancy between measured and predicted data. Meanwhile, the *AGD* is a measure of the average ratio between measured and predicted a_T data. As defined in the equation, the $\tilde{R}_i$ values are always greater or equal to unity. $\tilde{R}_i$ is equal to one when the predicted and measured a_T are identical. Thus the lowest possible value for *AGD* is 1. For instance, if it is 2, it means that the predicted a_T will be 2 (or 0.5) times the measured a_T.

Taking the range of r_i of 0.90–1.10 as an example, the LCPC method shows the best result, followed by the WLF, VTS, Arrhenius, Modified Kaelble and Log-Linear equations. A similar finding is observed with the use of *MNE* goodness-of-fit parameters. However, no different in terms of the *AGD* values could be observed on the unaged samples. The Arrhenius equation might produce a better fit of $|G^*|$ (or δ) master curves for low temperatures [34]. With one coefficient needing to be determined, the Arrhenius equation shows a low degree of freedom in its equation. At low temperatures, the activation energy, E_a, that associated with the Arrhenius equation varies. However, the E_a values become more constant as the temperatures increased [9]. Since the E_a values are relatively consistent, the Arrhenius equation is only reliant on temperature which explains why this equation becomes invalid at high temperatures. The use of one E_a value is obviously unable to yield a complete behaviour of $|G^*|$ and δ master curves of bituminous binders.

In general, the LCPC equation shows the best correlation between measured and predicted a_T of the r_i distribution in the range of r_i of 0.90–1.10 for the aged unmodified bitumens, as shown in Table 3. It is followed by the Modified Kaelble, VTS, WLF, and Arrhenius equations. As expected, the Log-Linear shows the least correlation in term of goodness-of-fitting statistical analysis. The breakdown of the TTSP could be related to the ageing process that results in increased of asphaltenes content. It is also interesting to note that the Modified Kaelble and LCPC methods show comparable results in terms of r_i and *MNE*, followed by the WLF, VTS, Arrhenius and Log-Linear equations for the aged PMBs. The WLF, Modified Kaelble, LCPC and VTS equations are well dispersed around the equality line for the aged bitumen-filler mastics. However, the

Table 4. Shifting Coefficients of the WLF Equation.

Unaged	Unmodified Bitumen		Bitumen-filler Mastics		PMBs	
	C1	C2	C1	C2	C1	C2
Average	22	125	12	107	17	158
Minimum	12	109	11	93	11	104
Maximum	46	162	14	130	51	479
Aged	Unmodified Bitumen		Bitumen-filler Mastics		PMBs	
	C1	C2	C1	C2	C1	C2
Average	15	131	13	114	17	135
Minimum	14	124	11	90	11	67
Maximum	16	150	21	190	39	304

Arrhenius and Log-Linear equations show the largest scatter in predicted results with small a_T values of r_i in the range of r_i of 0.90–1.10 for aged PMBs and bitumen-filler mastics. There is a dispersion of $|G^*|$ data for the aged bitumen-filler mastics at high temperatures, due to the influence of the material's granular skeleton, which renders the TTSP invalid for these materials [35].

It can also be inferred that as all the above methods are essentially empirical, they cannot be expected to be valid for all the material combinations [32]. The *AGD* parameter shows comparable results for most of the aged samples. This finding concludes that method is not always reliable at detecting the goodness-of-fit between measured and predicted a_T of bituminous binders, unaged and aged samples. Finally, it is worth mentioning that there are many possible solutions that have been used to find the goodness-of-fit statistical parameters. The methods explained in this section are limited and only include those that have been used by researchers and practitioners in the bitumen industry.

WLF Coefficients

Previous researchers have shown that the C_1 and C_2 values for unaged and aged bitumens can be taken as 19 and 92, respectively [24, 36-37]. However, the results from this study, as shown in Table 4, found that the values of C_1 and C_2 are inconsistent from one sample to the next. Similar results were obtained by Di Benedetto and co-workers [10-11] with the values for C_1 being more consistent than those for C_2. Generally, the WLF equation does not fit bitumen rheological data with the same set of constants above and below the softening point, where $|G^*|$ is increasingly dominated by viscous and elastic effects, respectively. Based on this argument, one might expect poor superposition of $|G^*|$ data taken over a frequency interval sufficiently wide as to include both glassy and viscous asymptotes for the master curve [20, 38]. Recently, Chailleux *et al.* [21] attempted to link the WLF coefficients to the physico-chemical state of bituminous binders. They found the C_2 parameter was linked to the thermal dependency of the materials with an increase in C_2 value with ageing.

Activation Energy

The activation energy, E_a, can be defined as a minimum energy required before any particular molecular movement can occur. Table 5 shows the E_a values calculated using Eq. (4) for a set of

Table 5. The E_a Values of Different Polymer Contents.

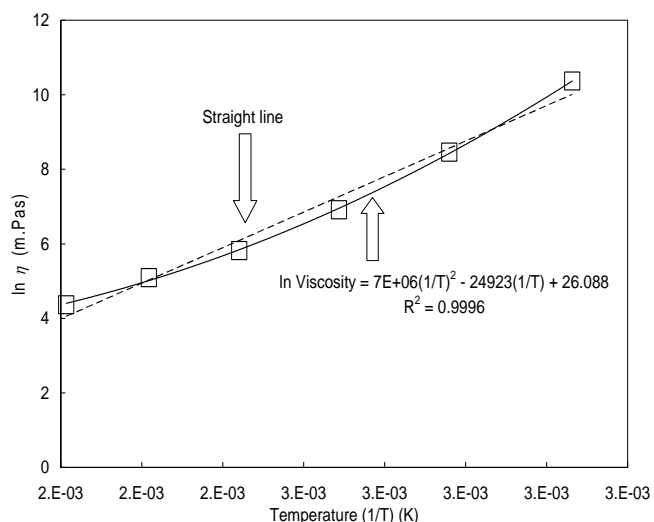| Temperature (K)	E_a (kJ/mol)						
	Unmodified	PMBs					
		EVA			SBS		
		3%	5%	7%	3%	5%	7%
283.15	168	187	199	203	183	184	196
288.15	160	182	195	193	175	172	192
308.15	165	164	179	175	157	162	164
318.15	158	162	178	170	156	160	159
328.15	152	158	173	179	150	157	157
338.15	146	156	167	177	145	152	150
348.15	141	150	166	185	140	145	145

Fig. 8. The ln η Versus Temperatures Curve of Unmodified Bitume.

unmodified bitumens and PMBs. In general, the E_a values are relatively constant for this set of binders with only a slight decrease with increasing temperature. However, results may actually reflect some testing (compliance) errors and also the occurrence of plastic deformation during testing at high temperatures. In addition, it is important to note that changing certain parameters, such as the type of bitumen, type and content of polymer modification, bitumen-filler mastics and ageing process will potentially alter the E_a values [39, 40].

In theory, a curve between a natural logarithmic of viscosity (ln η) and temperatures should produce a straight line to show that the E_a values are independent on temperatures. In this investigation, the viscosity of a 40/60 penetration grade bitumen was tested at a range of temperatures from 80 to 180°C. It is observed in Fig. 8 that the ln η versus temperatures is more conveniently presented in the form of a second order of polynomial fitting function rather than a straight line. A general form of equation that relates ln η and temperatures can be written as follows:

$$\ln \eta = a \times \left(1/T\right)^2 - b \times \left(1/T\right) + c \qquad (21)$$

where η is viscosity, T is temperature (K), a, b, and c are unknown coefficients. Not all chemical reactions will give a straight line particularly of materials like bitumens. It can be inferred that the E_a values of unmodified bitumens are varies and dependent on

temperatures. Similar observations might be expected from PMBs and bitumen-filler mastics as their behaviour are much more complicated compared to the unmodified bitumens.

Conclusions

For the range of temperatures from 5 to 75°C, the Generalised Logistic Sigmoidal Model is able to accurately model the complex modulus data obtained from LVE frequency sweep tests undertaken with a DSR. With the exception of the LCPC method, all the shift factor equations can be used together with this model to construct complex modulus master curves at an arbitrary selected reference temperature. The numerical, non-functional form shift function produces the most consistent set of results due to high degree of freedom and overall flexibility of this non-linear least squares fitting approach. The LCPC and WLF equations generally produced the best results compared to the numerical shift approach (predicted versus measured shift factor data) for all the material combinations studied, followed by the Modified Kaelble, VTS, Arrhenius and Log-Linear methods. As expected, the Log-Linear equation showed the lowest correlation with measured shift factor data, with this equation being more suitable for the construction of asphalt mixture complex modulus master curves.

The LCPC method, which is based on the Kramers-Kronig relationship, produced comparable a_T data with the numerical shift approach. However, this approach is highly reliant on consistent phase angle data and very sensitive to any compliance errors associated with the particular DSR machine. Results from this study showed that dispersions of a_T data normally occurred at changes between frequency sweep temperatures, particular the highest tested frequency at a particular temperature and the beginning of the frequency sweep (lowest tested frequency) at the next highest temperature. However, most of the equations are basically empirical and it is not expected that they will strictly obeyed by any materials

In terms of comparing the different shift factor functions and methods, both a graphical and a number of goodness-of-fit statistics were used. The graphical plots were able to visually observe the agreement between predicted and measured data, although this method is unreliable at detecting small changes in data. It is found that the R^2 and S_e/S_y parameters are not suitable for describing mismatches between predicted and experimental data. The R^2 is more applicable for linear models, while R^2 and S_e/S_y cannot be considered to be independent of each other. The average geometric

deviation (*AGD*) is also not always reliable at detecting goodness-of-fit even though it is meant for data scattered over a logarithmic scale. It is therefore recommended that the discrepancy ratio (r_i) and the mean normalized error (*MNE*) provide the best means of identifying the goodness-of-fit statistics for measured and predicted data associated with the shifting of rheological data over wide temperature and frequency domains.

References

1. Airey, G.D. (2002). Use of Black Diagrams to Identify Inconsistencies in Rheological Data, *Road Materials and Pavement Design*, 3(4), pp. 403–424.
2. Harrigan, E.T., Leahy, R.B., and Youtcheff, J.S. (1994). The SUPERPAVE Mix Design System Manual of Specifications, Test Methods and Practices, *SHRP-A-379*, Strategic Highways Research Program, National Research Council, Washington, DC, USA.
3. Rowe, G., Baumgardner, G., and Sharrock, M. (2009). Functional Forms for Master Curve Analysis of Bituminous Materials, *Proceedings of 7th International RILEM Symposium ATCBM09 on Advanced Testing and Characterization of Bituminous Materials*, 1, pp. 81–91, Rhodes, Greece.
4. Wada, Y. and Hirose, H. (1960). Glass Transition Phenomena and Rheological Properties of Petroleum Asphalt, *Journal of Physical Society of Japan*, 15(10), pp. 1885–1894.
5. Coleman, M.M. and Painter, P.C. (1997). *Fundamental of Polymer Science: An Introductory Text*, 2nd Edition, CRC Press, Florida, USA.
6. Kriz, P., Stastna, J., and Zanzotto, L. (2008). Physical Aging in Semi-Crystalline Asphalt Binders (with Discussion), *Journal of the Association of Asphalt Paving Technologists*, 77, pp. 795–826.
7. Goodrich, J.L. (1988). Asphalt and Polymer Modified Asphalt Properties Related to the Performance of Asphalt Concrete Mixes, *Proceedings of the Association of Asphalt Paving Technologists*, 57, pp. 116–175.
8. Airey, G.D. and Brown, S.F. (1998). Rheological Performance of Aged Polymer Modified Bitumens, *Journal of the Association of Asphalt Paving Technologists*, 67, pp. 66–100.
9. Pellinen, T.K., Witczak, M.W., and Bonaquist, R.F. (2002). Asphalt Mix Master Curve Construction using Sigmoidal Fitting Function with Non-Linear Least Squares Optimization Technique, *Proceedings of the 15th ASCE Engineering Mechanics Conference*, Columbia University, New York, USA.
10. Olard, F. and Di Benedetto, H. (2003). General "2S2P1D" Model and Relation between the Linear Viscoelastic Behaviours of Bituminous Binders and Mixes, *Road Materials and Pavement Design*, 4(2), pp. 185–224.
11. Olard, F., Di Benedetto, H., Eckmann, B., and Triquigneaux J.P. (2003). Linear Viscoelastic Properties of Bituminous Binders and Mixtures at Low and Intermediate Temperatures, *Road Materials and Pavement Design*, 4(1), pp. 77–107.
12. Witczak, M.W. and Bari, J. (2004). Development of A Master Curve (*E**) Database for Lime Modified Asphaltic Mixtures, Arizona State University, Tempe, Arizona, USA.
13. Shaw, M.T. and MacKnight, W.J. (2005). *Introduction to Polymer Viscoelasticity*, 3rd Edition, John Wiley & Sons, Inc. Hoboken, New Jersey, USA.
14. Ferry, J.D. (1980). *Viscoelastic Properties of Polymers*, 3rd Edition, John Wiley & Sons, Inc, New York, USA.
15. Airey, G.D. (2002). Rheological Evaluation of Ethylene Vinyl Acetate Polymer Modified Bitumens, *Construction and Building Materials*, 16(8), pp. 473–487.
16. Airey, G.D. (2003). Rheological Properties of Styrene Butadiene Styrene Polymer Modified Road Bitumens, *Fuel*, 82(14), pp. 1709–1719.
17. Airey, G.D., Liao, M.C., and Thom, N.H. (2006). Fatigue Behaviour of Bitumen-Filler Mastics, *Proceedings of the 10th International Conference on Asphalt Pavements, Quebec City, Canada*, 1, pp. 485–495.
18. Wu, J. and Airey, G.D. (2009). The Influence of Aggregate Interaction and Aging Procedure on Bitumen Aging, *ASTM Journal of Testing and Evaluation*, 37(5), pp. 402–409.
19. Williams, M.L., Landel, R.F., and Ferry, J.D. (1955). The Temperature-Dependence of Relaxation Mechanisms in Amorphous Polymers and Other Glass-Forming Liquids, *Journal of the American Chemical Society*, 77, pp. 3701–3706.
20. Dobson, G.R. (1969). The Dynamic Mechanical Properties of Bitumen, *Proceedings of the Association of Asphalt Paving Technologists*, 38, pp. 123– 139.
21. Chailleux, E., Ramond, G., Such, C., and de la Roche, C. (2006). A Mathematical-based Master Curve Construction Method Applied to Complex Modulus of Bituminous Materials, *Road Materials and Pavement Design*, 7, pp. 75–92.
22. Garcia, G. and Thompson, M.R. (2007). HMA Dynamic Modulus Predictive Models: A Review, *Research Report FHWA-ICT-07-2005*, Illinois Centre for Transportation, Illinois, USA.
23. Levenberg, E. and Shah, A. (2008). Interpretation of Complex Modulus Test Results for Asphalt Aggregate Mixes, *ASTM Journal of Testing and Evaluation*, 36(4), pp. 326–334.
24. Medani, T.O. and Huurman, M. (2003). Constructing the Stiffness Master Curves for Asphaltic Mixes, Report 7-01-127-3, Delft University and Technology, Netherland.
25. Mirza, M.W. and Witczak, M.W. (1995). Development of a Global Aging System for Short and Long Term Aging of Asphalt Cements, *Journal of the Association of Asphalt Paving Technologists*, 64, pp. 393–430.
26. Bonaquist, R. and Christensen, D.W. (2005). Practical Procedure for Developing Dynamic Modulus Master Curves for Pavement Structural Design, *Transportation Research Record*, No. 1929, pp. 208–217.
27. Morrison, F.A. (2005). Using the Solver Add-In in Microsft Excel. Online http:// www.chem.mtu.edu/~fmorriso /cm4650/Using_Solver_in_Excel.pdf, Last Accessed September, 2010.
28. Tran, N.H. and Hall, K.D. (2005). Evaluating the Predictive Equation in Determining Dynamic Moduli of Typical Asphalt Mixtures Used in Arkansas, *Electronic Journal of the Association of Asphalt Paving Technologists*, 74E.
29. Wu, B., Molinas, A. and Julien, P.Y. (2004). Bed-Material Load Computations for Non-Uniform Sediments, *Journal of Hydraulic Engineering*, 130(10), pp. 1002–1012.

30. Wu, B., Maren, D.S.V., and Li, L. (2008). Predictability of Sediment Transport in the Yellow River using Selected Transport Formulas, *International Journal of Sediment Research*, 23, pp. 283–298.

31. Molinas, A. and Wu, B. (2000). Comparison of Fractional Bed-Material Load Computation Methods in Sand-Bed Channels, *Earth Surface Processes and Landforms*, 25, pp. 1045–1068.

32. Dealy, J.M. and Larson, R.G. (2006). Structure and Rheology of Molten Polymers From Structure to Flow Behavior and Back Again. Hanser Publisher, Munich, Germany.

33. Valenkar, S.S. and Giles, D. (2007). How do I Know if My Phase Angles Are Correct? *Rheology Bulletin*, 76(2), pp. 8–20.

34. Zeng, M., Bahia, H.U., Zhai, H., Anderson, M.R., and Turner, P. (2001). Rheological Modeling of Modified Asphalt Binders and Mixtures, *Proceedings of the Association of Asphalt Paving Technologists*, 70, pp. 403–444.

35. Delaporte, B., Di Benedetto, H., Chaverot, P., and Gauthier, G. (2007). Linear Viscoelastic Properties of Bituminous Materials; from Binders to Mastics, *Journal of the Association of Asphalt Paving Technologists*, 76, pp. 455–494.

36. Christensen, D.W. and Anderson, D.A. (1992). Interpretation of Dynamic Mechanical Test Data for Paving Grade Asphalt, *Journal of the Association of Asphalt Paving Technologists*, 61, pp. 67–116.

37. Anderson, D.A., Christensen, D.W., Bahia, H.U., Dongré, R., Sharma, M.G., Antler, C.E., and Button, J. (1994). Binder Characterization and Evaluation, Volume 3: Physical Characterization, SHRP-A-369, National Research Council, Washington, DC, USA.

38. Jongepier, R. and Kuilman, B. (1969). Characteristics of the Rheology of Bitumens, *Proceedings of the Association of Asphalt Paving Technologists*, 38, pp. 98–122.

39. Salomon, D. and Zhai, H. (2002). Ranking Asphalt Binders by Activation Energy for Flow. Journal of Applied Asphalt Binder Techology, 2(2), pp. 52 – 60.

40. Salomon, D. and Zhai, H. (2004). Asphalt Binder Flow Activation Energy and its Significance for Compaction Effort. *Proceedings of 3rd Euroasphalt & Eurobitume Congress*, Book II, Paper 116, pp. 1754–1762.